Aquatic Toxicology 250 (2022) 106244

Contents lists available at ScienceDirect

Aquatic Toxicology

journal homepage: www.elsevier.com/locate/aqtox

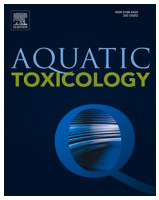

Environmental concentrations of a delorazepam-based drug impact on embryonic development of non-target *Xenopus laevis*

Chiara Fogliano [a], Chiara Maria Motta [a], Paola Venditti [a], Gianluca Fasciolo [a], Gaetana Napolitano [b], Bice Avallone [a,*], Rosa Carotenuto [a]

[a] Department of Biology, University of Naples Federico II, Naples, Italy
[b] Department of Science and Technology, University of Naples Parthenope, Naples, Italy

ARTICLE INFO

Keywords:
Environmental toxicity
FETAX test
Teratogenicity, Gene expression
Oxidative stress

ABSTRACT

Benzodiazepines, psychotropics drugs used for treating sleep disorders, anxiety and epilepsy, represent a major class of emerging water pollutants. As occurs for other pharmaceutical residues, they are not efficiently degraded during sewage treatment and persist in effluent waters. Bioaccumulation is already reported in fish and small crustaceans, but the impact and consequences on other "non-target" aquatic species are still unclear and nowadays of great interest. In this study, we investigated the effects of a pharmaceutical preparation containing the benzodiazepine delorazepam on the embryogenesis of *Xenopus laevis*, amphibian model species, taxa at high risk of exposure to water contaminants. Environmental (1 μg/L) and two higher (5 and 10 μg/L) concentrations were tested on tadpoles up to stage 45/46. Results demonstrate that delorazepam interferes with embryo development and that the effects are prevalently dose-dependent. Delorazepam reduces vitality by decreasing heart rate and motility, induces marked cephalic and abdominal edema, as well as intestinal and retinal defects. At the molecular level, delorazepam increases ROS production, modifies the expression of some master developmental genes and pro-inflammatory cytokines. The resulting stress condition significantly affects embryos' development and threatens their survival. Similar effects should be expected as well in embryos belonging to other aquatic species that have not been yet considered targets for these pharmaceutical residues.

1. Introduction

Benzodiazepines (BZDs), psychotropic drugs used for treating insomnia and anxiety (Argyropoulos and Nutt, 1999), are worldwide one of the most prescribed remedies (Schmitz, 2016; Nunes et al., 2019). Massive use and abuse (Votaw et al., 2019) result in a vast and constant release of these drugs and/or their active metabolites in the wastewater (Bade et al., 2020). Since they are not efficiently degraded during sewage treatment (Patel et al., 2019), BZDs accumulate in effluent waters and sediments (Klaminder et al., 2015; Lei et al., 2021), reaching concentrations ranging from μg/L to ng/L (Calisto and Esteves, 2009). As a consequence, BZDs represent nowadays an important class of emerging pollutants (Nunes et al., 2019) and therefore a potential environmental hazard, even at low concentrations, especially for aquatic species with which they inevitably come into contact (Klaminder et al., 2015). GABA receptors, targets for BZDs, are evolutionary very conserved, from bacteria (Guthrie et al., 2000) to animals (Furuhagen et al., 2014) and therefore large-scale effects are foreseeable. BZDs bioaccumulate in invertebrates (Lebreton et al., 2021a) and vertebrates, inducing relevant behavioral (Cerveny et al., 2020) and physiological alterations (Silva et al., 2020), including interferences with gene expression, enzymes activities (Oggier et al., 2010; Lebreton et al., 2021b) and oxidative stress (Ogueji et al., 2017).

The behavior and fate of BZDs in the aquatic environment are still not fully clear and so are the effects exerted on non-target species which may come accidentally into contact with these drugs. In particular, not very much is known about the effects on amphibians even if they are a class of vertebrates at high risk of exposure being bound to the aquatic environment both during embryonic development and adult life. In this study, therefore, we investigated the effects of a benzodiazepine delorazepam-based drug (DLZ) on the embryo development of a model species, *Xenopus laevis,* widely used in toxicology and environmental studies (Carotenuto et al., 2020; 2022).

Delorazepam, derivative of diazepam, is one of the benzodiazepines

* Corresponding author.
E-mail address: bice.avallone@unina.it (B. Avallone).

https://doi.org/10.1016/j.aquatox.2022.106244
Received 13 April 2022; Received in revised form 11 July 2022; Accepted 18 July 2022
Available online 20 July 2022

with the highest elimination half-life (80–115 h) and that produces a major active metabolite known as lorazepam that represents about 15 – 34% of the parent drug (Bareggi et al., 1988). Like all benzodiazepines, it has anxiolytic, skeletal muscle relaxant, and hypnotic properties (Bareggi et al., 1986; Moosmann and Auwärter, 2018).

Xenopus embryos were exposed to a largely consumed pharmaceutical product (oral drops) containing delorazepam at a concentration of 1 mg/ml. Preparation was used as it is, assuming that trace components are not relevant functionally or toxicologically. Preparation was diluted to a final concentration of DLZ of 1 μg/L, calculated considering the average concentration of different benzodiazepines in European waste and coastal waters (Fick et al., 2017; Calisto and Esteves, 2009). Two higher concentrations were also tested, 5 and 10 μg/L, for comparison and to mimic the simultaneous exposure to multiple BZDs occurring in nature.

The effects of the drug were determined by a modified version of the FETAX test and its conventional endpoints (Bernardini et al, 1994; Carotenuto et al., 2021): mortality, length, and occurrence of malformation, *in toto* and at the retinal level, proven target of embryo's toxicity (Hauptman et al., 1993; Simoniello et al., 2014). Following the occurrence of malformations, a preliminary gene expression analysis was also carried out to assess the possible influences of DLZ on the expression of early development genes, on the cytokine-mediated immunological response, and on the detoxification processes (see Table S1 and Carotenuto et al., 2021). In addition, in consideration of the sedative activity of DLZ, the impacts on embryonic swimming performance and heartbeat rate were determined. Changes in redox state were evaluated by ROS content analysis and by determining lipids oxidative damage, antioxidant enzymes activity (glutathione peroxidase and reductase), and i*n vitro* susceptibility to oxidants.

2. Materials and methods

2.1. Animals

Adult *Xenopus laevis*, obtained from Nasco (Fort Atkinson, Wisconsin, USA), were kept and used at the Department of Biology of the University of Naples, Federico II, according to the guidelines and policies dictated by the University Animal Welfare Office in agreement with international rules and strict accordance with the recommendations in the Guide for the Care and Use of Laboratory Animals of the National Institutes of Health of the Italian Ministry of Health. The protocol was approved by the Committee on the Ethics of Animal Experiments of the University of Naples Federico II (Permit Number: 2014/0017970). All procedures were performed according to Italian ministerial authorization (DL 116/92) and European regulations on the protection of animals employed for experimental and other scientific purposes. All surgical procedures were performed under tricaine (MS222, Sigma) and organized to minimize suffering. To obtain eggs, *X. laevis* females were injected in the dorsal lymphatic sac with 500 units of Gonase (AMSA) in amphibian Ringer solution (111 mM NaCl, 1.3 mM $CaCl_2$, 2 mM KCl, 0.8 mM $MgSO_4$, in 25 mM Hepes, pH 7.8). Fertilized eggs and embryos were obtained by standard insemination methods (Bernardini et al, 1994) and staged according to Nieuwkoop and Faber (1956).

2.2. Embryos' treatment

Three *in vitro* fertilizations were performed. For each fertilization, triplicate Petri dishes were set for controls (3 dishes containing 10 embryos for a total of 30 embryos) and delorazepam treatments (3 dishes containing 10 embryos for each concentration, for a total of 90 embryos). The experiment in triplicate produced a total of 360 embryos, 270 of which were exposed to the drug. The conventional FETAX assay was modified by anticipating the contact of the embryos with the drug at stage 4/8 cell, to emulate the environmental situation of contact with the drug and to study the effects on early development. 10 embryos at stage 4/8 for each treatment were selected for testing and placed in a 10 cm diam glass Petri dish containing 50 mL of FETAX solution (Frog Embryo Teratogenesis Assay-Xenopus pH 7.4; 106 mM NaCl, 11 mM $NaHCO_3$, 4 mM KCl, 1 mM $CaCl_2$, 4 mM $CaSO_4$, 3 mM $MgSO_4$), (Mouche et al., 2011).

For the treatment, a largely consumed pharmaceutical product was used. In form of oral drops, it contains the active principle delorazepam at a 1 mg/ml concentration and excipients in unspecified quantities (purified water, ethanol, glycasol N, glycerol, propylene glycol, sodium saccharin). Solutions were prepared by dissolving the drug in FETAX solution with different dilutions to obtain 1 μg/L, 5 μg/L, and 10 μg/L. Sibling embryos grown in FETAX solution were used as controls. All embryos were exposed up to stage 45/46 in a static condition, i.e., solutions were not renewed, so to determine the potentially embryotoxic effects of the delorazepam-based drug and/or its active metabolites. All the experiments were carried out at 21°C, under a 12 h light: 12 h dark photoperiod. The pH (7.4) of the solutions in the Petri dishes containing the embryos were checked daily. Embryo's survival and phenotypes were checked daily, and dead embryos were recorded and immediately removed.

2.3. Determination of embryo's phenotype, length, heart rate, and motility

For phenotype analysis, the survived embryos at stage 45/46 were anesthetized in FETAX containing 100 mg/L MS-222 (SIGMA) and placed under an MZ16F UV stereomicroscope equipped with a Leica DFC 300Fx camera. A photo of each class of most common malformation was taken in ventral, lateral, and dorsal positions. For length, heartbeat, and motility determination, thirty embryos from each treatment were randomly collected. A stereomicroscope equipped with an eyepiece micrometer was used to determine the length of the embryo. Heart rate was determined by counting the number of beats in a series of 30 s examinations, carried out in triplicate at a distance of 1 min (Carotenuto et al., 2016). For motility evaluation, the selected embryos were transferred into separate glass Petri dishes (diameter: 10 cm) containing 50 mL of FETAX solution, and let acclimatize for 5 min, protected by a black curtain from any possible disturbance exerted by the researcher. Single embryos were filmed for 60 s, and videos were analyzed by the software Tracker Video Analysis and Modeling Tool (Open-Source Physics). Speed and swimming activity data were normalized using the respective controls. The average velocity was determined as the distance traveled per second (cm/s), in the 60 s trials; time inactive (freeze) was quantified as average time (in seconds) spent resting, in the 60 s trials.

2.4. Histological analysis

Ten randomly selected embryos from each treatment were fixed in 2.5% glutaraldehyde and 4% paraformaldehyde in 0.1 M PBS pH 7.4 for 24h at 4°C, and post-fixed in 1% osmium tetroxide for 1 h at 4°C (Avallone et al., 2015). After washing in 0.1 M PBS pH 7.4 at 4°C, samples were dehydrated in ascending ethanol, and propylene oxide and embedded in Epon 812 (60°C, 48 h). Semi-thin sections (1.5 μm) of the eyes were cut and stained with 1% toluidine blue solution prepared in 1% sodium tetraborate buffer. For each embryo, 30 serial sections were examined with a Zeiss Axiocam camera applied to a Zeiss Axioskop microscope (Zeiss, Jena, Germany). Measurements of retina layers thickness and cells diameters were performed with the AxioVision software.

2.5. RNA and Real-Time PCR

For each treatment group, total RNA was extracted from a pool of 6 embryos with the Direct-zol RNA Mini Prep kit (ZymoResearch, Irvine, CA, USA) following the manufacturer's instruction and used for cDNA synthesis using the SuperScript Vilo cDNA synthesis kits (Life

Technologies Massachusetts, USA). Primers were designed using the software Primer 3 Plus (Table S1). Real-time PCR was performed using Power SYBR Green Master Mix kits (Life Technologies) using the 96-well optical reaction plate in 20 μL total reaction volume. Reactions were conducted on an AriaMx Real-time PCR System. The magnitude of change in gene expression relative to control was determined by the $2^{-\Delta\Delta Ct}$ method of Livak and Schmittgen (2001).

2.6. Redox state analysis

2.6.1. Preparations of homogenates

The analysis of redox state was performed on six samples for each experimental group. The embryos were finely minced and homogenized in a cold homogenization medium (HM, 220 mM mannitol, 70 mM sucrose, 1 mM EDTA, 0.1% fatty acid-free albumin, 10 mM Tris, pH 7.4) using a glass Potter-Elvehjem homogenizer set at 500 rpm for 1 min. Total protein content was measured by the biuret method and the homogenates were used for the following measures.

2.6.2. ROS content determination

The ROS content was measured according to Napolitano et al. (2022). In brief, 25 μg of homogenate proteins diluted in 200 μL of monobasic phosphate buffer were incubated for 20 min with 10 μM DCFH-DA at room temperature. Then, $FeCl_3$ was added to a final concentration of 100 μM, and the mixture was incubated for 30 min. The conversion of DCFH-DA to the fluorescent product DCF was measured using a multimode microplate reader (Synergy™ HTX Multimode Microplate Reader, BioTek) with excitation and emission wavelengths of 485 and 530 nm. Background fluorescence (conversion of DCFH to DCF in the absence of homogenate and mitochondria) was corrected with parallel blanks. ROS production was expressed as Relative Fluorescence Units per μg protein.

2.6.3. Oxidative damage to lipids

The level of lipid hydroperoxides (HPs) was used to measure the extent of the lipid peroxidative processes in the homogenates of the embryos. The measure was spectrophotometrically performed by using a system of two coupled enzymatic reactions catalyzed by glutathione peroxidase and glutathione reductase, respectively, in the presence of GSH and H_2O_2. The HPs levels were calculated by the rate of NADPH oxidation at 340nm and expressed as nmol NADPH oxidized/minutes per mg of proteins.

2.6.4. Activities of the antioxidant enzymes GPX and GR

GPX activity in 0.02 mg proteins of the homogenates was assayed at 25°C by using H_2O_2 as substrate according to Flohé and Günzler (1984). The reaction was spectrophotometrically followed at 340 nm by the oxidation of NADPH in the presence of GSH and GR. GR activity of 0.02 mg proteins of the homogenates was assayed at 25°C by measuring the rate of NADPH oxidation after the addition of GSSG. Each procedure was performed by using a multi-mode microplate reader (Synergy™ HTX Multi-Mode Microplate Reader, BioTek), and both enzymes' activities were expressed as nmol NADPH oxidized/minutes per mg of proteins.

2.6.5. In vitro susceptibility to oxidants

The *in vitro* susceptibility of homogenates to oxidants was evaluated by the change in hydroperoxide levels induced by treatment of 1 mg of homogenate proteins/mL with Fe and ascorbate (Fe/As), at concentrations of 100/1000 μM, for 10 min at room temperature (Venditti et al., 2016). The reaction was stopped by the addition of 0.2% 2.6-di-t-butyl-p-cresol (BHT) and the hydroperoxide levels were evaluated as previously described.

2.6.6. Cytochrome oxidase activity (COX)

COX activity of 0.1 mg proteins of the homogenate was polarographically determined at 25°C by using a respirometer Hansatech (Hansatech Instruments Ltd, United Kingdom). The measure was performed in 1.0 mL of buffer solution (30μM Citc 3131, 10 mM Sodium Malonate, 75 mM Hepes, 4 μM Rotenone, 0.5 mM 2.4-dinitrophenol, pH 7.4) after membranes solubilization with 1% Lubrol and in presence of a mixture of TMPD plus Ascorbate (30 mM plus 400mM). COX activity was expressed as μmol O/min per mg of proteins.

2.7. Statistical analysis

Data were processed with GraphPad-Prism 8 software (GraphPad Software, Inc., San Diego, CA, USA). The survival distributions in control and experimental groups were assessed in terms of significance using the Mantel-Cox test. To evaluate differences in heartbeat, length, motility, and oxidative stress among groups, the data were checked for compliance with parametric tests, then One-Way ANOVA followed by Tukey's pairwise comparison tests were performed. For Real-Time PCR, statistical significance was determined using Two-Way ANOVA with the Bonferroni test. Data were expressed as mean ± SD; probability was considered statistically significant at $p< 0.05$ (*), very significant at $p< 0.01$ (**) and at $p<0.001$ (***), and extremely significant at $p<0.0001$ (****).

3. Results

3.1. Embryo survival and body malformations

The embryos grown in presence of DLZ showed a significant dose-dependent increase in mortality ($p<0.0001$; Table S2, Fig. 1A): the percent of death reached 32.2% in 1 μg/L DLZ, 44.4% in 5 μg/L and 53.3% 10 μg/L DLZ. In controls, mortality remained at 11.1%. Control embryos showed an average length of 0.97 mm. No significant variations were registered in embryos exposed to DLZ at 1 and 5 μg/L while, in 10 μg/L treatment, a moderate but significant decrease in length was observed if compared to control and 1 μg/L (0.87 mm; $p<0.05$; Fig. 1B).

The incidence of malformations also follows a dose-dependent trend (Table S3). Control embryos showed a low rate of malformation, 3.7%, and anomalies consisted of a moderate and diffused swelling. In presence of DLZ, the percentages of malformations raised to 21.3% after 1 μg/L exposition and to 62.0% and 69.0% in embryos exposed to 5 or 10 μg/L.

Different types of malformations were common to the three dosages used, albeit with different frequencies (Table S3). Diffuse edema was the most common (61.5 to 74.2%), a condition making it impossible to distinguish the cephalic from the abdominal region (Fig. 2E, F). The head edema was the second most represented abnormal condition (16.1 to 38.5%) where, although the presence of abdominal swelling (Fig. 2C, D), the cephalic area was distinguishable (Fig. 2C, D). A bent tail condition was also occasionally observed (9.7%) but only in 5 μg/L embryos (Fig. 2H).

In control embryos the intestine appeared well organized, properly convoluted (Fig. 2B); in contrast, in DLZ treated embryos it appeared immature (Table S3), misfolded, apparently elongated, and/or dilated (Fig. 2D-F), often with clearly anomalous loops (Fig. 2F). The edema was frequently so consistent to cause an outbreak of the abdominal wall, with consequent extrusion of part of the intestine (Fig. 2G). In embryos with the bent tail condition, the immaturity of the intestine folding was a constant condition (Fig. 2H).

Body alterations were often accompanied by an alteration in the presence and/or distribution of the dorsal pigment (Fig. 2C, E) if compared to the control (Fig. 2A).

3.2. Retinal defects

The microscopic analyses of the control eyes (Fig. 3A) showed a typical differentiating retina. Ganglion cells (GCL) were organized in a monolayer, the inner plexiform layer (IPL) appeared a thick and dense

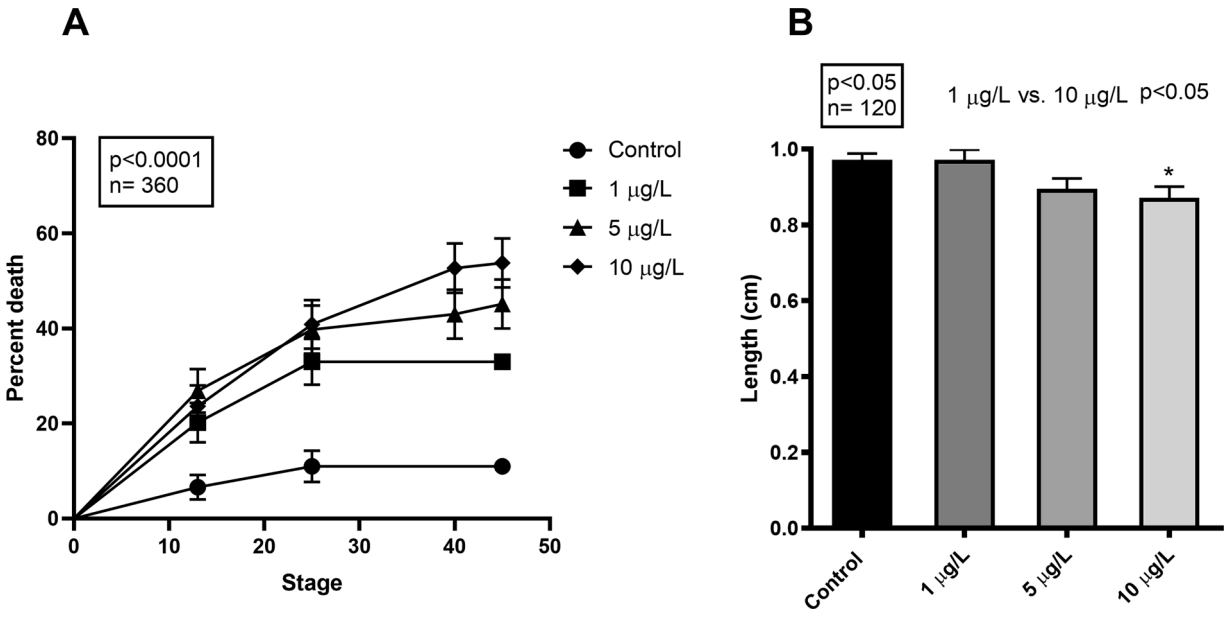

Fig. 1. Mortality and length in *Xenopus laevis* embryos exposed to delorazepam. (A) Mortality percentage significantly increases at all the concentrations and in all stages examined. Chi-square test for trend $p<0.0001$. (B) Significant growth retardation in embryos exposed to 10 μg/L if compared to control and 1 μg/L mean length. Chi-square test for trend $p<0.05$. Data are means ± SD; total number of embryos examined (n); Statistic Unit = 12. * $p<0.05$; ** $p<0.01$; *** $p<0.001$.

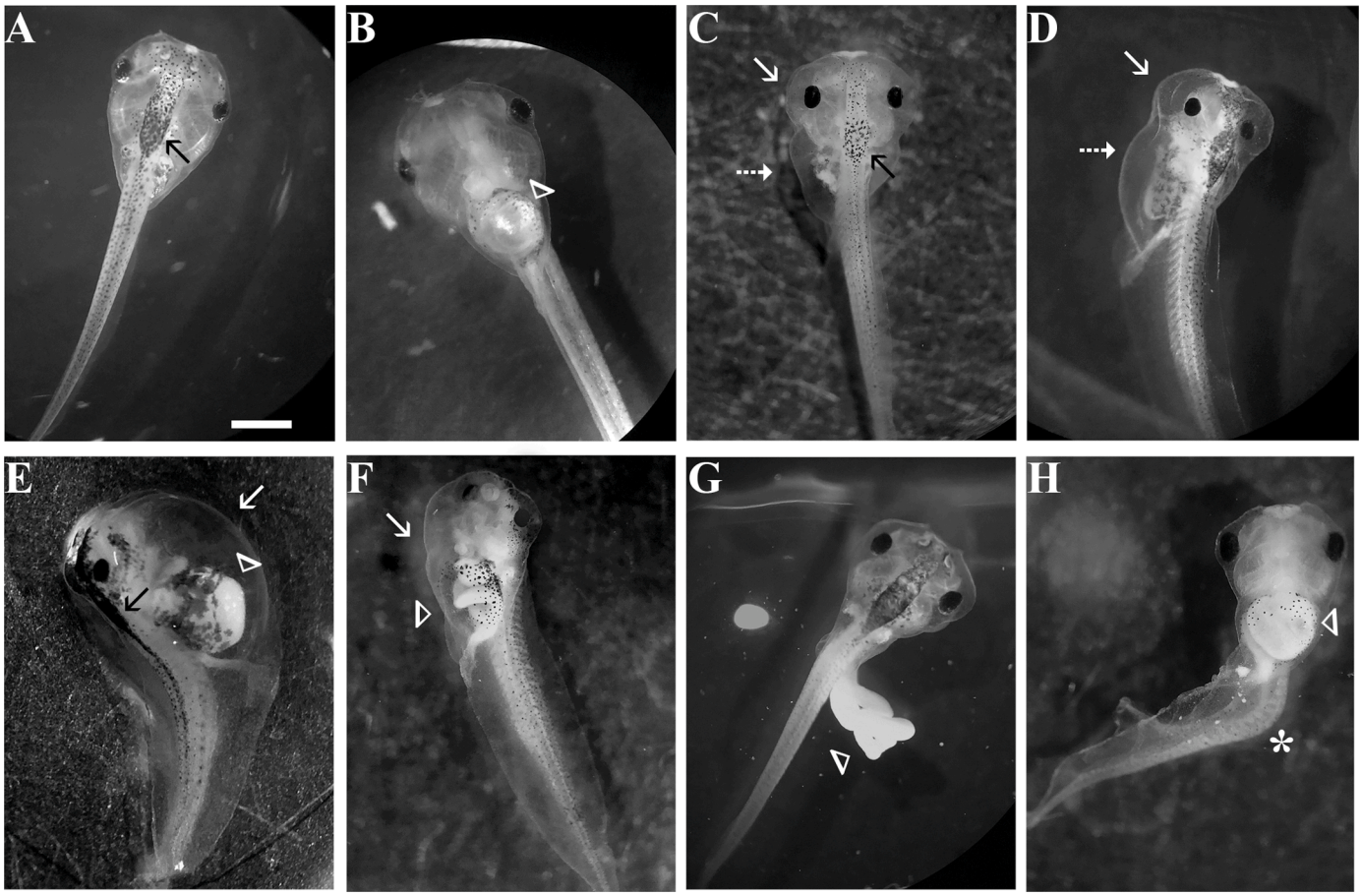

Fig. 2. Altered phenotypes in *Xenopus laevis* embryos exposed to delorazepam. (A) Dorsal and (B) ventral view of control embryo displaying the typical gross morphology with spiralized intestine (arrowhead). Notice the correct distribution of the dorsal pigment (black arrow); (C) Dorsal and (D) lateral view of embryos after exposition to delorazepam; head (arrow) and abdominal (dot arrow) edema, immature intestine (arrowhead), and reduced dorsal pigment (black arrow). (E-F) Lateral view of diffuse edema (arrow) with the presence of an immature intestine (arrowhead) and increased dorsal pigmentation (black arrow); (G) Leaking of the intestine (arrowhead) following the outbreak of abdominal edema; (H) Bent tail condition (asterisk) with immature intestine (arrowhead). Bar = 1.25mm.

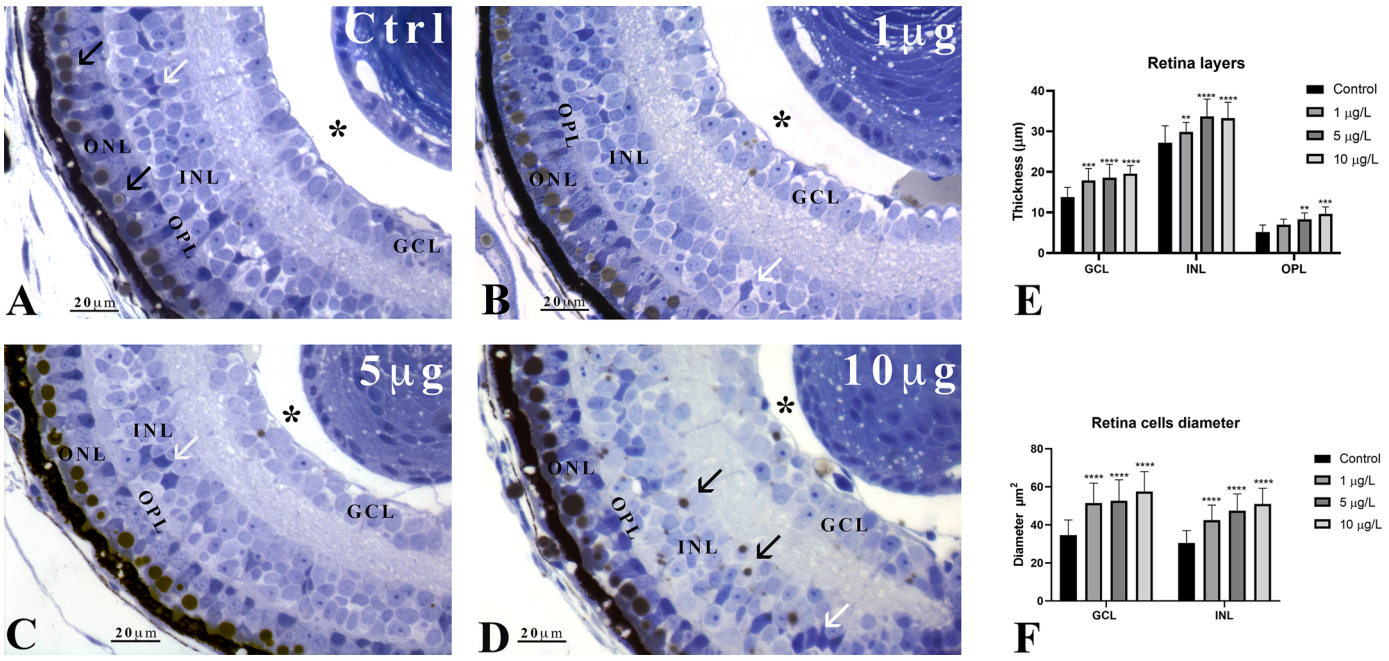

Fig. 3. Histological section of the retina of *Xenopus laevis* embryos treated with delorazepam. (A) Control; typical retinal organization with a monolayered GLC, an INL with dispersed Muller cells (white arrows), and oil drops in inner segments of cones (black arrows). Vitreous chamber (asterisk). (B-C) Increase in GCL, INL, and OPL thickness and marked decrease of the vitreous chamber (*). (D) GCL is multi-layered, the INL loosely organized with increased Muller cells (white arrows) and oil droplets (black arrows). (E and F) Dose-dependent increase in retinal layers thickness and retinal cells diameters in GLC, INC, and OPL. Data are means ± SD; $^{**}p<0.01$; $^{****}p<0.0001$.

reticulum of fibrils. The inner nuclear layer (INL) was multilayered, with tightly packed cells among which Muller cells were recognizable by the denser cytoplasm. The outer plexiform layer (OPL) was barely visible below a thick outer nuclear layer (ONL). It was characterized by the presence of large oil droplets, in the inner segment of cones photoreceptors, and by the contact with a regular pigmented epithelium. After exposure to DLZ, the thickness of the different layers (Fig. 3E) and cells size (Fig. 3F) significantly increased. At the environmental concentration of 1 µg/L, GCL and INL are thicker, ganglion cells and inner nuclear layer cells are larger and disarranged (Fig. 3B) if compared to controls. Increasing the dose to 5 µg/L (Fig. 3C) or 10 µg/L (Fig. 3D) caused a further dose-dependent increase in cells diameters (Fig. 3F) and layers thickness (Fig. 3E). This latter alteration was particularly evident in GCL, becoming multilayered, and in OPL, becoming distinguishable between INL and ONL. Significant changes are also observed in cells organization. In the INL, cells appeared loosely arranged and Muller cells increased in number, especially at 10 µg/L treatment. As a consequence, the retina appeared disorganized (Fig. 3C, D), thicker and the volume of the vitreous chamber markedly reduced (Fig. 3B-D). Moreover, oil drops were more numerous, bigger, and dispersed in the entire retina (Fig. 3B-D). No significant morphological changes were detected in the inner plexiform layer (IPL).

3.3. Bradycardia and impaired swimming performance

No differences were registered in the heartbeat rate between control

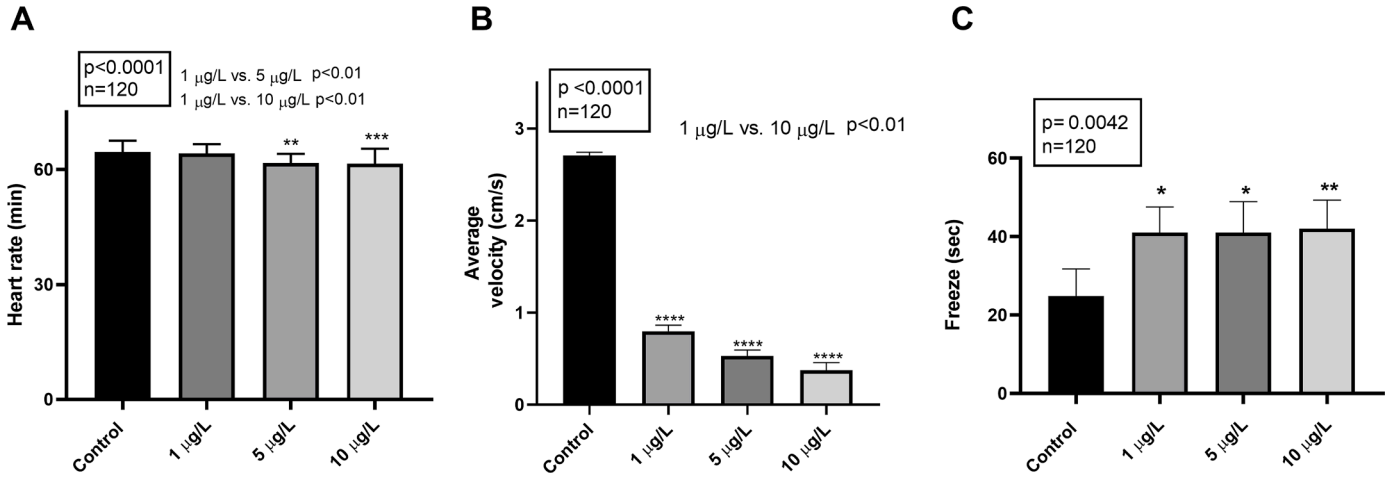

Fig. 4. Heart rate and swimming performance in *Xenopus laevis* embryos exposed to delorazepam. (A) Dose-dependent bradycardia in embryos exposed at 5 and 10 µg/L. Chi-square test for trend $p<0.0001$. (B) Dose-dependent decrease in swimming speed of the treated embryos. Chi-square test for trend $p<0.0001$. (C) Significant increase in time spent resting (freeze) during the 60-second trials. Chi-square test for trend $p=0.0042$. Data are reported as means ± SD; total number of embryos examined (n); $^{*}p<0.05$; $^{**}p<0.01$; $^{****}p<0.0001$.

embryos and embryos exposed to 1 μg/L DLZ: in both groups, an average frequency of 65 beats per minute was reported. A statistically significant decrease was observed in embryos exposed to 5 and 10 μg/L in which the average frequency reduced to 61 beats per minute (p <0.001; Fig. 4A). A significant decrease was also observed among the treaties (p<0.01).

Under normal conditions, swimming was inconstant, characterized by a burst in which the average speed was 2.85 ± 1.44 cm/s (Fig. 4B). The activity was followed by a short period of stasis during which the embryos were completely steady (Fig. 4B). However, when stimulated, the embryos immediately started moving. In the treated embryos, the average speed progressively and significatively decreases with increasing DLZ dosage: from 0.79 ± 0.42 cm/s at the environmental concentration (p<0.0001), to 0.62 ± 0.41 at 5 μg/L (p<0.0001) to 0.55 ± 0.36 at 10 μg/L (p<0.0001). A significant decrease was also observed between embryos treated with 1 μg/L and 10 μg/L (p<0.01). In addition, during the stasis, a prolonged stimulus was needed to restart the animal and, when swimming was finally resumed, it was slower.

Even the rest times, if compared to the controls (average 4 s every 60 s of activity), increased considerably after DLZ exposure, no matter the dose, lasting on average 41 s (Fig. 4C).

3.4. Altered genes expression

Results indicated that DLZ at the environmental dose of 1 μg/L induced a significant downregulation of *bmp4* and *egr2* (p<0.001), *fgf8* (p<0.01), and *pax6* (p<0.05). At 5 μg/L, *bmp4* and *fgf8* were normally expressed while *rax1* (p<0.0001) and *egr2* (p<0.001) were overexpressed and *sox9* and *pax6* significantly downregulated (p<0.0001). The highest dose of 10 μg/L induced overexpression of *bmp4* (p<0.0001), *egr2* and *rax1* (p<0.0001) while *sox9* and *pax6* remained downregulated (p<0.0001). *fgf8* levels were not modified (Fig. 5A).

Pro-inflammatory *tnfα* and *il1b* genes were already over-expressed at 1 μg/L (p<0.01 and p<0.0001), further increasing at the higher dosages (p<0.0001). *p65* showed a slight increase in expression at 1 and 5 μg/L, significantly raising at 10 μg/L (p<0.05). For the *abcb1* gene, the expression showed a gradual increase up to 5 μg /L (p<0.0001) and a decrease at 10 μg/L (p<0.0001) (Fig. 5B).

3.5. ROS content, oxidative damage of lipids, and antioxidant enzymes activity

ROS content significantly increases after exposure to delorazepam with the highest levels registered in 5 μg/L and 10 μg/L treatments (Fig. 6A). Treatments also induce a dose-dependent increase in lipid hydroperoxides levels (Fig. 6B). Both glutathione peroxidase (Fig. 7A) and glutathione reductase (Fig. 7B) activities increased after DLZ exposure, raising to the highest levels at 10 μg/L. In addition, all treated groups showed increased susceptibility to oxidants, particularly in the presence of a maximum concentration of delorazepam (Fig. 7C). The cytochrome oxidase activity (COX) remained unaffected by treatment with delorazepam (Fig. S1).

4. Discussion

Data collected demonstrate that DLZ profoundly influences early development in *Xenopus*. The benzodiazepine is confirmed sedative (Hollis and Boyd, 2005), as indicated by decreased heart rate and reduced locomotory performance, two effects depending on binding to GABA receptors of central nervous system (Zahner et al., 2007; Hollis and Boyd, 2005). DLZ is also confirmed teratogenic and able to alter gene expression (McElhatton, 1994; Pasbakhsh et al., 2013) and cause oxidative stress.

Concerning morphological anomalies, in mammalian embryos, BDZs reduce birth weight and affect head development, eyes, ears, brain, and mouth in particular (Pasbakhsh et al., 2013; Tandon and Mulvihill, 2009). In *Xenopus* embryos, the head gross morphology was apparently normal but the expression of developmental genes controlling neurulation, *sox9, egr2, pax6,* and *rax1*, was altered suggesting interference with nervous system development. In particular, the altered expression of *sox9* suggests a dysregulation of neural plate cells multipotency (Scott et al., 2010) while the altered expression of *egr2* indicates an alteration in Schwann cells development (Duong and Svaren, 2019). Altered *pax6* indicates potential interference with telencephalon dorso-ventral and anterior-posterior patterning, with the specification of neuronal subtypes, neuronal migration and axonal projection (Matsumoto and Osumi, 2008).

The hypothesis of DLZ induced nervous system damage is supported

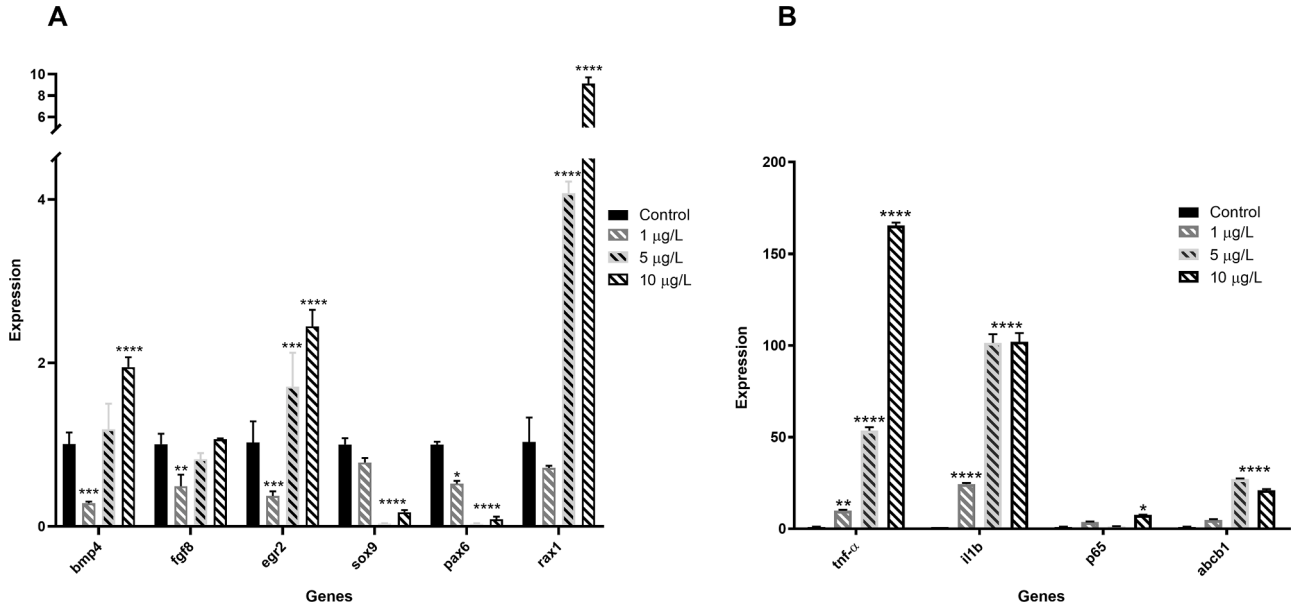

Fig. 5. Changes in gene expression in *Xenopus laevis* embryos exposed to delorazepam. (A) Early developmental genes expression was always downregulated at environmental doses, and up or downregulated at higher doses if compared to control expression. (B) Pro-inflammatory cytokines and *abcb1* genes tend to be overexpressed in the treated embryos. Data are means ± SD. *p<0.05; **p<0.01; ***p<0.001; ****p<0.0001.

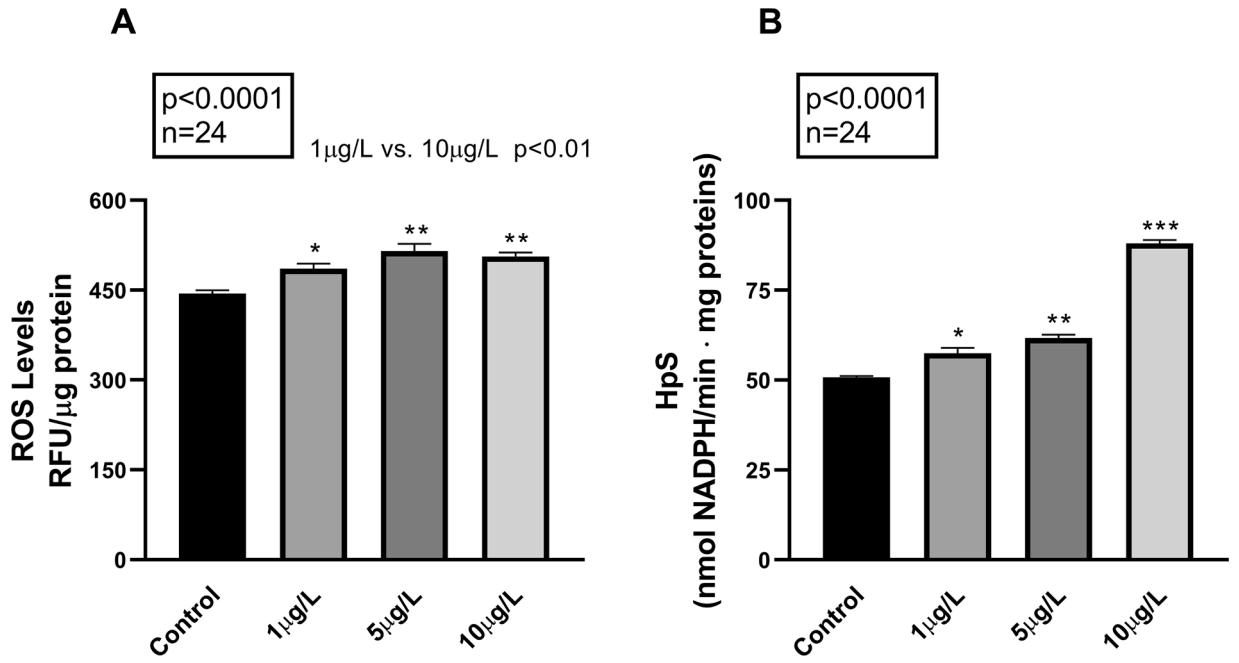

Fig. 6. Analysis of ROS content and oxidative damage to lipids in *Xenopus laevis* embryos homogenates. (A) ROS production increases at the environmental dose and raises further after 5 and 10 μg/L treatments. (B) Dose-dependent increase of the lipid hydroperoxides levels. Chi-square test for trend $p<0.0001$. Data are means ± SD. Total number of embryos examined (n); Statistic Unit = 12. *$p<0.05$; **$p<0.01$; ***$p<0.001$.

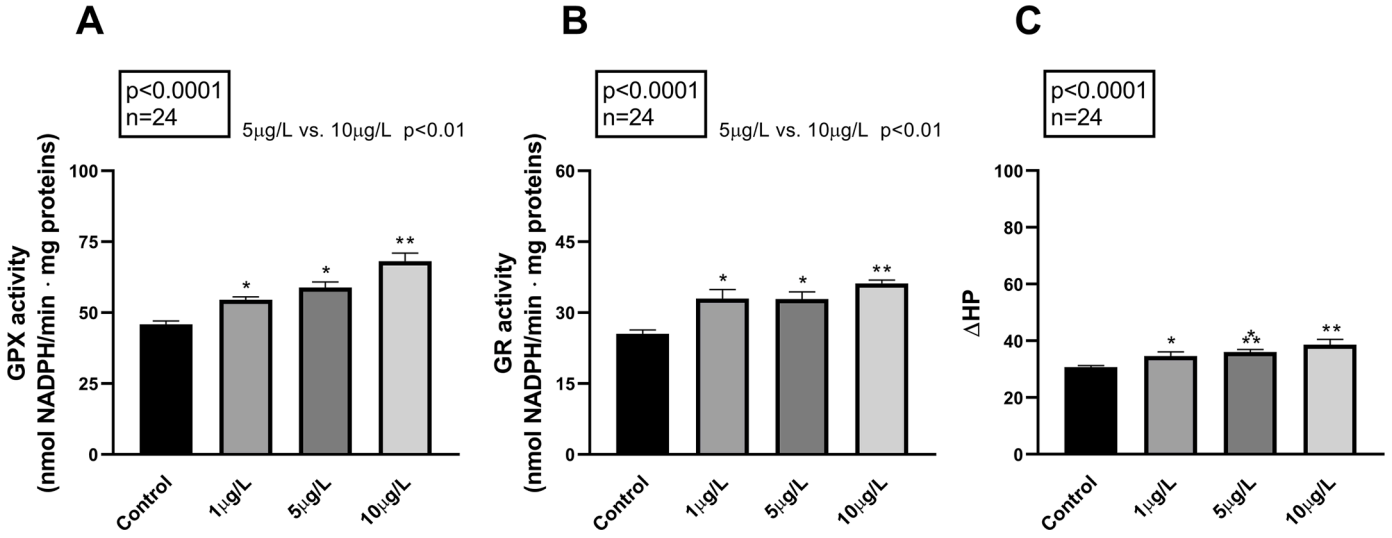

Fig. 7. Activities of glutathione peroxidase GPX (A) and reductase GR (B), and *in vitro* susceptibility to oxidants ΔHP (C) in *Xenopus laevis* embryos homogenates. A dose-dependent increase is noticed for all parameters analysed. Chi-square test for trend p<0.0001. Data are means ± SD. Total number of embryos examined (n). Statistic Unit = 12. *$p<0.05$; **$p<0.01$; ***$p<0.001$.

by two further pieces of evidence. The first is the observed changes in pigmentation, a process also depending on *sox9* and *egr2*: the former controls neural crest cell differentiation (Tussellino et al., 2016) and melanocytes number while the latter controls melanocytes distribution in the skin (Aoki et al., 2003). The second evidence is DLZ interference with retinal development. The downregulation of *sox9* and *pax6* can be responsible for the observed alteration in the organization of the inner plexiform and ganglion cells layers, the two in which GABAa receptors were already expressed at the time of treatment (Soklnick et al., 1980). The action would have been exerted by interfering with retinal progenitors' fate (Hsieh and Yang, 2009). Further investigation is necessary to prove the interference and to test nervous system development and functionality; however, anomalies similar to those observed in *Xenopus* were already registered in lizard embryos exposed to cadmium. In this species, retinal damage and *pax6* dysregulation were associated with anomalies in the mesencephalic roof, due to changes in rate and time of cell proliferation (Simoniello et al., 2014).

Eye damages were not particularly severe but together with altered oil droplets size and distribution can prelude to aniridia, cataracts, or corneal defects (Nakayama et al., 2015) and impaired visual performance. Not to neglect the fact that ganglion cells normally produce a neuroactive steroid controlling the inhibitory transmission (Guarneri et al., 1995). DLZ might have interfered with its release or function, therefore opening a number of new research questions.

Data from the retina are particularly interesting also for another aspect. *pax6* under expression accounts for the observed anticipation of

retinal precursors differentiation (Philips et al., 2005) and, in particular, for the increased number of differentiating Muller cells (Zhu et al., 2013). However, it does not explain the increased thickness of the ganglion cells layer. The observed effects can be attributed to increased proliferation, but this usually relates to a *pax6* overexpression (Simoniello et al., 2014). A suggestive hypothesis comes therefore from these contrasting data: that DLZ has different, region-specific effects in the retina mimicking what is already demonstrated in the brain (Musavi and Kakkar, 1998).

Evidence of DLZ teratogenicity also comes from gut deformities. Very frequent and particularly evident, they are indicative of a delayed winding of gut loops (Chalmers and Slack, 1998), a common response in *Xenopus* embryos intoxication (Carotenuto et al., 2022). Delay can be associated with the observed over-expression of *bmp4*, a gene involved in gut specification, regionalization, and differentiation (Fu et al., 2006). Based on this evidence, exposed *Xenopus* embryos would not feed properly, and the reduced size would support the hypothesis. The smaller size of treated embryos however can also depend on the altered expression of *fgf8*, a gene involved in embryonic axes determination and elongation (Dorey and Amaya, 2010).

Coming to the causes of the observed alterations, they are probably multiple and interconnected. Oxidative stress certainly has a primary role as both cause and effect. No information is available on DLZ but another benzodiazepine, the diazepam, has proven pro-oxidative effects (Musavi and Kakkar, 1998). ROS production can activate the MAPK signaling pathways, which further activates several inflammatory cytokines (Park et al., 2011). In *Xenopus* embryos, overexpression of *tnfα, il1b,* and *p65* is registered which explains edema and developmental changes. In addition, ROS acts as a second messenger and, by regulating key transcription factors, both positively and negatively can affect cell signaling, proliferation, and death affecting embryonic development (Dennery, 2007). Is not a case that ROS represents a very early and sensitive biomarker of amphibian developmental toxicity (Rizzo et al., 2007).

Another factor must be taken into consideration: the benzodiazepine peripheral receptors or PBR/TSPO, a transmembrane protein located in the outer mitochondrial membrane. The TSPO binds benzodiazepines with micromolar affinity, is evolutionary highly conserved (Bonsack and Sukumari-Ramesh, 2018), is present in all tissues, and is already expressed in embryos (Papadopoulos et al., 1997). The receptor controls growth and differentiation, gene expression (Yasin et al., 2017) and the immune response (Betlazar et al., 2020). All these effects are compatible with the effects observed in *X. laevis* embryos. In addition, being oxygen sensor, TSPO can control ROS production and mitochondrial functionality (activity), thus contributing to oxidative stress production.

TSPO, by controlling mitochondrial functionality control cell bioenergetics (Betlazar et al., 2020), and, as a consequence, is a potential responsible for the reduced embryo motility (Alelwani et al., 2020). However, cytochrome oxidase activity, *in vitro* correlating to the maximum aerobic capacity of the tissues, did not change in DLZ treated embryos. Therefore, the observed decreased heart rate and reduced locomotory performance would depend exclusively on a drop in blood pressure and sympathetic nerve activity induced by DLZ potentiation of GABAergic inhibition (Zahner et al., 2007; Snyder et al, 2000). As expected, the increase in ROS triggered a protective response.

As in other species, *Xenopus* embryos activated low molecular weight antioxidants and antioxidants enzymes, such as GPX and GR. Glutathione reductase catalyzes the reduction of glutathione disulfide (GSSG) to the sulfhydryl form glutathione (GSH), which is a critical molecule in resisting oxidative stress and maintaining the reducing environment of the cell. The enzyme glutathione peroxidase utilizes reduced glutathione to neutralize hydrogen peroxide and lipid hydroperoxides (Napolitano et al., 2021). These enzymatic activities have been reported to increase after diazepam exposure (Ogueji et al., 2017). However, the antioxidant enzyme activity was not sufficient to counteract the DLZ-induced increase in ROS level. Indeed, in *Xenopus* embryos, the capacity to face *in vitro* oxidative stress was reduced in DLZ treated animals, especially at the higher concentrations. This could explain why, though different DLZ concentrations increase ROS content to the same extent, at the higher DLZ concentrations oxidative damage was more consistent. On the other hand, the reduced capacity to face *in vitro* oxidative stress at the highest DLZ concentration can depend on the reduced expression of the *abcb1* gene, a member of the ABC cassette multi-xenobiotic pump involved in detoxifying mechanisms and, in the extrusion from the cells of unmodified exogenous compounds (Guo et al., 2020).

5. Conclusion

Data evidentiate that benzodiazepines such as delorazepam if released in the environment, interfere with amphibians' embryos development. Morphological, behavioral, and molecular alterations are induced, and these significantly impair embryo survival. Oxidative stress is certainly involved but up to now, it is unclear if ROS is a cause or a consequence of the observed alterations. Most probably the effects depend on a synergic action of ROS, GABA, and TSPO receptors but only further studies will fully clarify the delorazepam way of action. The relevance of the observed effects indicates that immediate attention must be paid to this class of contaminants and that they should be monitored during environmental risk assessment.

Funding

This research did not receive any specific grant from funding agencies in the public, commercial, or not-for-profit sectors.

CRediT authorship contribution statement

Chiara Fogliano: Investigation, Methodology, Formal analysis, Writing – original draft, Visualization. **Chiara Maria Motta:** Writing – original draft, Writing – review & editing, Supervision, Conceptualization, Validation. **Paola Venditti:** Supervision, Writing – review & editing, Validation. **Gianluca Fasciolo:** Methodology. **Gaetana Napolitano:** Methodology, Data curation. **Bice Avallone:** Supervision, Data curation, Visualization, Validation. **Rosa Carotenuto:** Supervision, Data curation, Visualization, Validation.

Declaration of Competing Interest

The authors declare that they have no known competing financial interests or personal relationships that could have appeared to influence the work reported in this paper.

Supplementary materials

Supplementary material associated with this article can be found, in the online version, at doi:10.1016/j.aquatox.2022.106244.

References

Alelwani, W, Elmorsy, E, Kattan, SW, Babteen, NA, Alnajeebi, AM, Al-Ghafari, A, Carter, WG., 2020. Carbamazepine induces a bioenergetics disruption to microvascular endothelial cells from the blood-brain barrier. Toxicol. Lett. 333, 184–191. https://doi.org/10.1016/j.toxlet.2020.08.006. Oct 15.

Argyropoulos, S.V., Nutt, D.J., 1999. The use of benzodiazepines in anxiety and other disorders. Eur. Neuropsychopharmacol. 9 (6), S407–S412. https://doi.org/10.1016/s0924-977x(99)00052-8. Suppl.

Aoki, Y., Saint-Germain, N., Gyda, M., Magner-Fink, E., Lee, Y.H., Credidio, C., Saint-Jeannet, J.P., 2003. Sox10 regulates the development of neural crest-derived melanocytes in Xenopus. Dev. Biol. 259 (1), 19–33. https://doi.org/10.1016/s0012-1606(03)00161-1.

Avallone, B., Crispino, R., Cerciello, R., Simoniello, P., Panzuto, R., Motta, C.M., 2015. Cadmium effects on the retina of adult Danio rerio. C.R. Biol. 338 (1), 40–47. https://doi.org/10.1016/j.crvi.2014.10.005.

Bade, R., Ghetia, M., White, J.M., Gerber, C., 2020. Determination of prescribed and designer benzodiazepines and metabolites in influent wastewater. Anal. Methods 12 (28), 3637–3644. https://doi.org/10.1039/d0ay00560f.

Bareggi, S.R., Nielsen, N.P., Leva, S., Pirola, R., Zecca, L., Lorini, M., 1986. Age-related multiple-dose pharmacokinetics and anxiolytic effects of delorazepam (chlordesmethyldiazepam). Int. J. Clin. Pharmacol. Res. 6 (4), 309–314.
Bareggi, S.R., Truci, G., Leva, S., Zecca, L., Pirola, R., Smirne, S., 1988. Pharmacokinetics and bioavailability of intravenous and oral chlordesmethyldiazepam in humans. Eur. J. Clin. Pharmacol. 34 (1988), 109–112. https://doi.org/10.1007/BF01061430.
Bernardini, G., Vismara, C., Boracchi, P., Camatini, M., 1994. Lethality, teratogenicity and growth inhibition of heptanol in Xenopus assayed by a modified frog embryo teratogenesis assay-Xenopus (FETAX) procedure. Sci. Total Environ. 151 (1), 1–8. https://doi.org/10.1016/0048-9697(94)90480-4.
Betlazar, C., Middleton, R.J., Banati, R., Liu, G.J., 2020. The Translocator Protein (TSPO) in Mitochondrial Bioenergetics and Immune Processes. Cells, 9 (2), 512. https://doi.org/10.3390/cells9020512.
Bonsack, F., Sukumari-Ramesh, S., 2018. TSPO: an evolutionarily conserved protein with elusive functions. Int. J. Mol. Sci. 19 (6), 1694. https://doi.org/10.3390/ijms19061694.
Calisto, V., Esteves, V.I., 2009. Psychiatric pharmaceuticals in the environment. Chemosphere 77 (10), 1257–1274. https://doi.org/10.1016/j.chemosphere.2009.09.021.
Carotenuto, R., Capriello, T., Cofone, R., Galdiero, G., Fogliano, C., Ferrandino, I., 2020. Impact of copper in Xenopus laevis liver: histological damages and atp7b downregulation. Ecotoxicol. Environ. Saf. 188, 109940 https://doi.org/10.1016/j.ecoenv.2019.109940.
Carotenuto, R., Fogliano, C., Rienzi, M., Siciliano, A., Salvatore, M.M., De Tommaso, G., Benvenuto, G., Galdiero, E., Guida, M., 2021. Comparative toxicological evaluation of tattoo inks on two model organisms. Biology 10 (12), 1308. https://doi.org/10.3390/biology10121308.
Carotenuto, R., Tussellino, M., Mettivier, G., Russo, P., 2016. Survival fraction and phenotype alterations of Xenopus laevis embryos at 3 Gy, 150 kV X-ray irradiation. Biochem. Biophys. Res. Commun. 480 (4), 580–585. https://doi.org/10.1016/j.bbrc.2016.10.095.
Carotenuto, R., Tussellino, M., Ronca, R., Benvenuto, G., Fogliano, C., Fusco, S., Netti, P. A., 2022. Toxic effects of SiO2NPs in early embryogenesis of Xenopuslaevis. Chemosphere 289, 133233. https://doi.org/10.1016/j.chemosphere.2021.133233.
Cerveny, D., Brodin, T., Cisar, P., McCallum, E.S., Fick, J., 2020. Bioconcentration and behavioral effects of four benzodiazepines and their environmentally relevant mixture in wild fish. Sci. Total Environ. 702, 134780 https://doi.org/10.1016/j.scitotenv.2019.134780.
Chalmers, A.D., Slack, J.M., 1998. Development of the gut in Xenopus laevis. Developmental dynamics : an official publication of the. Am. Assoc. Anatomists 212 (4), 509–521. https://doi.org/10.1002/(SICI)1097-0177(199808)212:4<509::AID-AJA4>3.0.CO;2-L.
Dennery, P.A., 2007. Effects of oxidative stress on embryonic development. Birth Defects Res. Part C Embryo Today 81 (3), 155–162. https://doi.org/10.1002/bdrc.20098.
Dorey, K., Amaya, E., 2010. FGF signalling: diverse roles during early vertebrate embryogenesis. Development 137 (22), 3731–3742. https://doi.org/10.1242/dev.037689.
Duong, P., Svaren, J. (2019). Chromatin Signaling and Neurological Disorders. ISBN 978-0-12-813796-3.
Fick, J., Brodin, T., Heynen, M., Klaminder, J., Jonsson, M., Grabicova, K., Randak, T., Grabic, R., Kodes, V., Slobodnik, J., Sweetman, A., Earnshaw, M., Barra Caracciolo, A., Lettieri, T., Loos, R., 2017. Screening of benzodiazepines in thirty European rivers. Chemosphere 176, 324–332. https://doi.org/10.1016/j.chemosphere.2017.02.126.
Flohé, L., Günzler, W.A., 1984. Assays of glutathione peroxidase. Methods Enzymol. 105, 114–121. https://doi.org/10.1016/s0076-6879(84)05015-1.
Fu, M., Vohra, B.P., Wind, D., Heuckeroth, R.O., 2006. BMP signaling regulates murine enteric nervous system precursor migration, neurite fasciculation, and patterning via altered Ncam1 polysialic acid addition. Dev. Biol. 299 (1), 137–150. https://doi.org/10.1016/j.ydbio.2006.07.016.
Furuhagen, S., Fuchs, A., Lundström Belleza, E., Breitholtz, M., Gorokhova, E., 2014. Are pharmaceuticals with evolutionary conserved molecular drug targets more potent to cause toxic effects in non-target organisms? PLoS One 9 (8), e105028. https://doi.org/10.1371/journal.pone.0105028.
Guarneri, P., Guarneri, R., Cascio, C., Piccoli, F., Papadopoulos, V., 1995. gamma-Aminobutyric acid type A/benzodiazepine receptors regulate rat retina neurosteroidogenesis. Brain Res. 683 (1), 65–72. https://doi.org/10.1016/0006-8993(95)00343-o.
Guo, B., Xu, Z., Yan, X., Buttino, I., Li, J., Zhou, C., Qi, P., 2020. Novel ABCB1 and ABCC Transporters Are Involved in the Detoxification of Benzo(α)pyrene in Thick Shell Mussel, Mytilus Coruscus. Front. Mar. Sci. 7, 119. https://doi.org/10.3389/fmars.2020.00119.
Guthrie, G.D., Nicholson-Guthrie, C.S., Leary Jr, H.L., 2000. A bacterial high-affinity GABA binding protein: isolation and characterization. Biochem. Biophys. Res. Commun. 268 (1), 65–68. https://doi.org/10.1006/bbrc.1999.1960.
Hauptman, O., Albert, D.M., Plowman, M.C., Hopfer, S.M., Sunderman Jr, F.W., 1993. Ocular malformations of Xenopus laevis exposed to nickel during embryogenesis. Ann. Clin. Lab. Sci. 23 (6), 397–406.
Hollis, D.M., Boyd, S.K., 2005. Distribution of GABA-like immunoreactive cell bodies in the brains of two amphibians, Rana catesbeiana and Xenopus laevis. Brain Behav. Evol. 65 (2), 127–142. https://doi.org/10.1159/000082981.
Hsieh, Y.W., Yang, X.J., 2009. Dynamic Pax6 expression during the neurogenic cell cycle influences proliferation and cell fate choices of retinal progenitors. Neural Dev. 4, 32. https://doi.org/10.1186/1749-8104-4-32.
Klaminder, J., Brodin, T., Sundelin, A., Anderson, N.J., Fahlman, J., Jonsson, M., Fick, J., 2015. Long-Term Persistence of an Anxiolytic Drug (Oxazepam) in a Large Freshwater Lake. Environ. Sci. Technol. 49 (17), 10406–10412. https://doi.org/10.1021/acs.est.5b01968.
Lebreton, M., Malgouyres, J.M., Carayon, J.L., Bonnafé, E., Géret, F., 2021a. Effects of the anxiolytic benzodiazepine oxazepam on freshwater gastropod reproduction: a prospective study. Ecotoxicology 30 (9), 1880–1892. https://doi.org/10.1007/s10646-021-02453-y.
Lebreton, M., Sire, S., Carayon, J.L., Malgouyres, J.M., Vignet, C., Géret, F., Bonnafé, E., 2021b. Low concentrations of oxazepam induce feeding and molecular changes in Radix balthica juveniles. Aquat. Toxicol. 230, 105694 https://doi.org/10.1016/j.aquatox.2020.105694.
Lei, H.J., Yang, B., Ye, P., Yang, Y.Y., Zhao, J.L., Liu, Y.S., Xie, L., Ying, G.G., 2021. Occurrence, fate and mass loading of benzodiazepines and their transformation products in eleven wastewater treatment plants in Guangdong province, China. Sci. Total Environ. 755 (Pt 2), 142648 https://doi.org/10.1016/j.scitotenv.2020.142648.
Livak, K.J., Schmittgen, T.D., 2001. Analysis of relative gene expression data using real-time quantitative PCR and the 2(-Delta Delta C(T)) Method. Methods (San Diego. Calif.) 25 (4), 402–408. https://doi.org/10.1006/meth.2001.1262.
Matsumoto, Y., Osumi, N., 2008. Role of Pax6 in the developing central nervous system. Brain Nerve Shinkei kenkyu no shinpo 60 (4), 365–374.
McElhatton, P.R., 1994. The effects of benzodiazepine use during pregnancy and lactation. Reprod. Toxicol. (Elmsford, N.Y.), 8 (6), 461–475. https://doi.org/10.1016/0890-6238(94)90029-9.
Moosmann, B., Auwärter, V., 2018. Designer benzodiazepines: another class of new psychoactive substances. Handb. Exp. Pharmacol. 252, 383–410. https://doi.org/10.1007/164_2018_154.
Mouche, I., Malesic, L., Gillardeaux, O., 2011. FETAX assay for evaluation of developmental toxicity. Methods Mol. Biol. 691, 257–269. https://doi.org/10.1007/978-1-60761-849-2_15.
Musavi, S., Kakkar, P., 1998. Diazepam induced early oxidative changes at the subcellular level in rat brain. Mol. Cell. Biochem. 178 (1-2), 41–46. https://doi.org/10.1023/a:1006834706117.
Nakayama, T., Fisher, M., Nakajima, K., Odeleye, A.O., Zimmerman, K.B., Fish, M.B., Yaoita, Y., Chojnowski, J.L., Lauderdale, J.D., Netland, P.A., Grainger, R.M., 2015. Xenopus pax6 mutants affect eye development and other organ systems, and have phenotypic similarities to human aniridia patients. Dev. Biol. 408 (2), 328–344. https://doi.org/10.1016/j.ydbio.2015.02.012.
Napolitano, G., Fasciolo, G., Magnacca, N., Goglia, F., Lombardi, A., Venditti, P., 2022. Oxidative damage and mitochondrial functionality in hearts from KO UCP3 mice housed at thermoneutrality. J. Physiol. Biochem. https://doi.org/10.1007/s13105-022-00882-9. Advance online publication. h t t p s://doi.org/10.1007/s13105-022-00882-9.
Napolitano, G, Fasciolo, G, Venditti, P., 2021 Nov 17. Mitochondrial management of reactive oxygen species. Antioxidants (Basel) 10 (11), 1824. https://doi.org/10.3390/antiox10111824.
Nieuwkoop, P.D., Faber, J., 1956. Normal Table of Xenopus laevis (Daudin): A Systematical and Chronologica Survey of the Development from the Fertilized Egg till the End of Metamorphosis. Amsterdam, North-Holland.
Nunes, C.N., Dos Anjos, V.E., Quináia, S.P., 2019. Are there pharmaceutical compounds in sediments or in water? Determination of the distribution coefficient of benzodiazepine drugs in aquatic environment. Environ. Poll. (Barking, Essex : 1987) 251, 522–529. https://doi.org/10.1016/j.envpol.2019.05.015.
Oggier, D.M., Weisbrod, C.J., Stoller, A.M., Zenker, A.K., Fent, K., 2010. Effects of diazepam on gene expression and link to physiological effects in different life stages in zebrafish Danio rerio. Environ. Sci. Technol. 44 (19), 7685–7691. https://doi.org/10.1021/es100980r.
Ogueji, E.O., Iheanacho, S.C., Nwani, C.D., Christian, E.M., Okeke, O.C., Usman, I.B., 2017. Toxicity of diazepam on lipid peroxidation, biochemical and oxidative stress indicators on liver and gill tissues of African catfish Clarias gariepinus (Burchell, 1822). Int. J. Fish. Aquat. Stud. 5 (3), 114–123.
Papadopoulos, V., Amri, H., Boujrad, N., Cascio, C., Culty, M., Garnier, M., Hardwick, M., Li, H., Vidic, B., Brown, A.S., Reversa, J.L., Bernassau, J.M., Drieu, K., 1997. Peripheral benzodiazepine receptor in cholesterol transport and steroidogenesis. Steroids 62 (1), 21–28. https://doi.org/10.1016/s0039-128x(96)00154-7.
Park, K.R., Nam, D., Yun, H.M., Lee, S.G., Jang, H.J., Sethi, G., Cho, S.K., Ahn, K.S., 2011. β-Caryophyllene oxide inhibits growth and induces apoptosis through the suppression of PI3K/AKT/mTOR/S6K1 pathways and ROS-mediated MAPKs activation. Cancer Lett. 312 (2), 178–188. https://doi.org/10.1016/j.canlet.2011.08.001.
Pasbakhsh, P., Mehrannia, K., Barbarestani, M., 2013. The teratogenic effects of Lorazepam on the organogenesis of the rat fetus. Acta Med. Iran 1 (1), 29–32, 41.
Patel, M., Kumar, R., Kishor, K., Mlsna, T., Pittman Jr, C.U., Mohan, D, 2019. Pharmaceuticals of emerging concern in aquatic systems: chemistry, occurrence, effects, and removal methods. Chem. Rev. 119 (6), 3510–3673. https://doi.org/10.1021/acs.chemrev.8b00299.
Philips, G.T., Stair, C.N., Young Lee, H., Wroblewski, E., Berberoglu, M.A., Brown, N.L., Mastick, G.S., 2005. Precocious retinal neurons: Pax6 controls timing of differentiation and determination of cell type. Dev. Biol. 279 (2), 308–321. https://doi.org/10.1016/j.ydbio.2004.12.018.
Rizzo, A.M., Adorni, L., Montorfano, G., Rossi, F., Berra, B., 2007. Antioxidant metabolism of Xenopus laevis embryos during the first days of development. Comparative biochemistry and physiology. Part B Biochem. Mol. Biol. 146 (1), 94–100. https://doi.org/10.1016/j.cbpb.2006.09.009.
Schmitz, A., 2016. Benzodiazepine use, misuse, and abuse: a review. Mental Health Clin. 6 (3), 120–126. https://doi.org/10.9740/mhc.2016.05.120.

Scott, C.E., Wynn, S.L., Sesay, A., Cruz, C., Cheung, M., Gomez Gaviro, M.V., Booth, S., Gao, B., Cheah, K.S., Lovell-Badge, R., Briscoe, J., 2010. SOX9 induces and maintains neural stem cells. Nat. Neurosci. 13 (10), 1181–1189. https://doi.org/10.1038/nn.2646.

Silva, A., Nilin, J., Loureiro, S., Costa-Lotufo, L.V., 2020. Acute and chronic toxicity of the benzodiazepine diazepam to the tropical crustacean Mysidopsis juniae. An. Acad. Bras. Cienc. 92 (1), e20180595 https://doi.org/10.1590/0001-3765202020180595.

Simoniello, P., Trinchella, F., Filosa, S., Scudiero, R., Magnani, D., Theil, T., Motta, C.M., 2014. Cadmium contaminated soil affects retinogenesis in lizard embryos. J. Exp. Zool. Part A Ecol. Genet. Physiol. 321 (4), 207–219. https://doi.org/10.1002/jez.1852.

Snyder, M.J, Watson, S., Peeke, H.V.S., 2000. Lobster locomotor activity as a measure of GABAA receptor modulation. Mar. Freshw. Behav. Physiol. 34 (1), 37–51. https://doi.org/10.1080/10236240009379058.

Soklnick, P., Paul, S., Zatz, M., Eskay, R., 1980. 'Brain-specific'benzodiazepine receptors are localized in the inner plexiform layer of rat retina. Eur. J. Pharmacol. 66 (1), 133–136.

Tandon, A., Mulvihill, A., 2009. Ocular teratogens: old acquaintances and new dangers. Eye 23, 1269–1274. https://doi.org/10.1038/eye.2009.30.

Tussellino, M., Ronca, R., Carotenuto, R., Pallotta, M.M., Furia, M., Capriglione, T., 2016. Chlorpyrifos exposure affects fgf8, sox9, and bmp4 expression required for cranial neural crest morphogenesis and chondrogenesis in Xenopus laevis embryos. Environ. Mol. Mutagen. 57 (8), 630–640. https://doi.org/10.1002/em.22057.

Venditti, P, Napolitano, G, Barone, D, Pervito, E, Di Meo, S., 2016. Vitamin E-enriched diet reduces adaptive responses to training determining respiratory capacity and redox homeostasis in rat heart. Free Radic. Res. 50 (1), 56–67. https://doi.org/10.3109/10715762.2015.1106530.

Votaw, V.R., Geyer, R., Rieselbach, M.M., McHugh, R.K., 2019. The epidemiology of benzodiazepine misuse: a systematic review. Drug Alcohol Depend. 200, 95–114. https://doi.org/10.1016/j.drugalcdep.2019.02.033.

Yasin, N., Veenman, L., Singh, S., Azrad, M., Bode, J., Vainshtein, A., Caballero, B., Marek, I., Gavish, M., 2017. Classical and Novel TSPO Ligands for the Mitochondrial TSPO Can Modulate Nuclear Gene Expression: Implications for Mitochondrial Retrograde Signaling. Int. J. Mol. Sci. 18 (4), 786. https://doi.org/10.3390/ijms18040786.

Zahner, M.R., Li, D.P., Pan, H.L., 2007. Benzodiazepine inhibits hypothalamic presympathetic neurons by potentiation of GABAergic synaptic input. Neuropharmacology 52 (2), 467–475. https://doi.org/10.1016/j.neuropharm.2006.08.024.

Zhu, Y., Carido, M., Meinhardt, A., Kurth, T., Karl, M.O., Ader, M., Tanaka, E.M., 2013. Three-dimensional neuroepithelial culture from human embryonic stem cells and its use for quantitative conversion to retinal pigment epithelium. PLoS One 8 (1), e54552. https://doi.org/10.1371/journal.pone.0054552.